Hindawi
Geofluids
Volume 2023, Article ID 5299919, 11 pages
https://doi.org/10.1155/2023/5299919

Research Article

Prediction of Grade Classification of Rock Burst Based on PCA-SSA-PNN Architecture

Zhenyi Wang,[1] **Yalei Wang**,[2] **and Xiaoliang Jin**[1]

[1]*School of Architectural Engineering, Zhengzhou University of Industrial Technology, Zhengzhou 451100, China*
[2]*Department of Civil Engineering, Shanghai University, Shanghai 200444, China*

Correspondence should be addressed to Zhenyi Wang; wzyizg@163.com

Received 24 March 2023; Revised 7 May 2023; Accepted 26 May 2023; Published 13 June 2023

Academic Editor: Qingchao Li

The uncertainty and complexity of rock burst brings great difficulties to the prediction of rock burst grades. In order to estimate the risk grades of rock burst, an integrated method combining principal component analysis (PCA) and sparrow search algorithm (SSA) with probabilistic neural network (PNN) was proposed. Considering that the in situ stress of rock mass, the strength of rock, and the strength of rock mass are the key influencing factors of rock bursts, the maximum in situ stress σ_{max}, maximum tangential stress σ_θ, rock strength σ_{ci}, rock mass strength σ_{cm}, and three rock burst evaluation indexes ($\sigma_\theta/\sigma_{ci}$, σ_{ci}/σ_{max}, and σ_{cm}/σ_{max}) were selected to constitute the rock burst grade evaluation index system. Forty-three groups of rock burst engineering data were gathered. After preprocessing the rock burst data using PCA, four of the new linearly independent indexes PCA_1, PCA_2, PCA_3, and PCA_4 were obtained for estimating rock burst grades. The SSA was utilized to optimize the smoothing factor in the PNN. Using PCA-SSA-PNN-based architecture, a new multi-index rock burst grade prediction method was proposed. The results from the new multi-index rock burst grade prediction method were compared with those from single- and multi-index prediction methods. It shows that the predictions from the multi-index rock burst prediction methods are closer to the actual rock burst grades than that from the single-index rock burst prediction methods; compared with other multi-index rock burst prediction methods, the prediction accuracy of PCA-SSA-PNN is greater (up to 90%) and more available in the prediction of rock burst grades. The results presented herein may provide reference for the rock burst warning.

1. Introduction

Rock burst is a kind of dynamic failure phenomenon which often occurs in the high ground stress area of deep buried tunnels. When the mechanical equilibrium state of rock mass is broken, the accumulated energy in the rock mass is released in a sudden and violent form, resulting in a dynamic instability phenomenon [1–5]. The accurate assessment of rock burst grade classification is an important content of rock burst prevention measures.

The prediction methods of rock burst grade used in practical engineering are usually based on rock strength, such as the Russenes criterion [6], Erlang Mountain criterion [7], and Barton criterion (Barton et al. [8]). Furthermore, in recent years, some scholars have further studied the rock burst prediction method also based on the rock strength. For example, Afraei et al. [9] analyzed the contribution rate of rock burst influencing factors to rock burst grade prediction and found that maximum tangential stress and uniaxial compressive strength of rock significantly contributed to rock burst grade prediction; He et al. [10] modified the previous rock burst grade prediction method by introducing the gradient stress and recognized that the range of the rock strength stress ratios used for rock burst grade prediction was not uniform; Wu et al. [11] put forward the rock burst criterion of Lalin railway tunnel, and compared with the Russenes criterion and Erlang Mountain criterion, the rock burst criterion of Lalin railway tunnel is more consistent with the actual situation of Lalin railway; Wang et al. [12] established a rock burst prediction model based on rock mechanical properties and in situ stress, which could be reliably applied to rock burst prediction. These above prediction

methods of rock burst grade consider the stress condition and mechanical properties of rock well and promote the research of rock burst prediction method.

However, the occurrence of an actual rock burst is more closely related to rock mass structure and strength, and there are some reports about predicting rock burst using rock mass structure and strength. For example, Qiu et al. [13] discussed the influence of rock mass structure on the velocity of flying rock when rock burst occurred and realized that floor deflection is an important focal mechanism that causes rock velocity and serious rock burst damage; Chen et al. [14] and Ma et al. [15] considered the impact of rock mass integrity on rock burst and found that the strength of rock mass is the main controlling factor for the prediction of rock burst grade; Du et al. [16] analyzed the influence of structural plane strength on rock burst and held that structural plane strength is the main factor to judge whether instantaneous rock burst or hysteretic rock burst occurs in rock mass; Mohamad et al. [17] considered that the joint spacing and apertures are the main causes that determine the number and distance of flying rocks as rock burst occurs; Feng et al. [18] and Zhou et al. [19] believed that rock mass structure is an important factor affecting the occurrence of rock burst, and the structural surface where rock burst occurs is mostly rigid surface. These above researches take the rock mass structure as the important factor of inducing rock burst, which is consistent with the actual situation.

In practice, most of the rock burst grade classification prediction methods based on the strength of rock materials or rock mass were based the single-index methods, and these methods were usually summarized from the specific engineering cases with the relatively less evaluation information. Considering the actual complexity, many scholars adopted the multi-index method to estimate the rock burst grade. For example, Zhou et al. [20] considered that genetic algorithm and particle swarm optimization algorithm could speed up the parameter optimization search of support vector machine (SVM), and the proposed method of rock burst grade prediction has strong robustness; Dong et al. [21] found that compared with SVM, the random forest algorithm had a lower misjudgment rate of rock burst grade; Wang et al. [22] established a multi-index method for rock burst prediction based on the fuzzy matter-element theory, information entropy theory, and proximity rule and found that the established method is more reliable than the traditional method; Zhang et al. [23] made a comprehensive prediction of rock burst based on the rock elastic energy index, rock strength, and principal stress, which could make up for the deficiency of single-index rock burst prediction method; Li et al. [24] proposed a rock burst prediction network based on genetic algorithm and extreme learning machine, and the prediction results show that the maximum relative error of the proposed method is 4.71%; Xu et al. [25, 26] put forward a new rock burst grade evaluation using the ideal point theory, and the error rate is 5%, and the average crossover error rate is 13.33%; Liang et al. [27] found that gradient-boosted decision tree algorithm could be applied to short-term rock burst prediction with an accuracy of more than 90%; Meng et al. [28] believed that BP (back propagation) neural network prediction and least square method may reduce the influence of subjective judgment on the prediction results and could obtain the prediction results in the first time; Chen et al. [29] utilized the Bayesian method to estimate the rock burst grade and found that Bayesian statistical learning model has robustness and generalization in rock burst risk assessment; Gao et al. [30] held that the radial basis neural network optimized by hybrid particle swarm optimization algorithm may take into account individual optimization and global optimization and could predict the rock burst grade correctly and effectively; Gong et al. [31] established a deep learning rock burst prediction model based on dropout and Adam algorithm, and the model avoids the problem of determining index weights and is completely data-driven; Liu et al. [32] found that the rock burst prediction network based on histogram gradient-enhanced tree algorithm still has a high prediction ability for incomplete rock burst data, with an accuracy of nearly 80%. In these above researches, machine learning and deep learning methods were adopted to establish a multi-index rock burst grade prediction network, and the accuracy of the prediction results was significantly improved than that of the single-index rock burst prediction method. The multi-index rock burst grade prediction methods could consider the influencing factors of rock burst in many aspects, reduce the interference of human factors, and make the prediction result more close to the actual situation.

Actually, the multi-index rock burst prediction methods may be used to reveal the mechanism of rock burst in more detail. However, the existing multi-index-based predictions usually focused on the rock strength and ignored the influence of rock mass strength. For the high complexity and unpredictability of a rock burst, it is necessary to conduct a new multi-index evaluation method of rock burst grade considering the rock mass strength. In this study, the field data of a tunnel in western China and the case data of diversion tunnel project in Pakistan [33] and Erlangshan tunnel project in China [7, 34] were used as the data set for rock burst grade evaluation. The data set was then divided into training set and test set. The principal component analysis (PCA) method was furthermore used both to reduce the dimension of the rock burst data set and to eliminate the linear correlation between different indexes. The sparrow search algorithm was also conducted to optimize the smoothing factor in the probabilistic neural network (PNN). The prediction results from the improved PNN algorithm were thereafter compared with those from other existing rock burst prediction methods, including single- and multi-index rock burst prediction methods.

2. PCA-SSA-PNN-Based Architecture

2.1. Structure of PNN. Probabilistic neural network (PNN) is a kind of network structure based on radial basis function proposed by Specht in 1990 [35], mainly composing of input layer, pattern layer, summation layer, and output layer as shown in Figure 1. The PNN has the characteristics of fast convergence, high stability, and no local optima and is suitable for rock burst grade classification. The PNN is briefly described below.

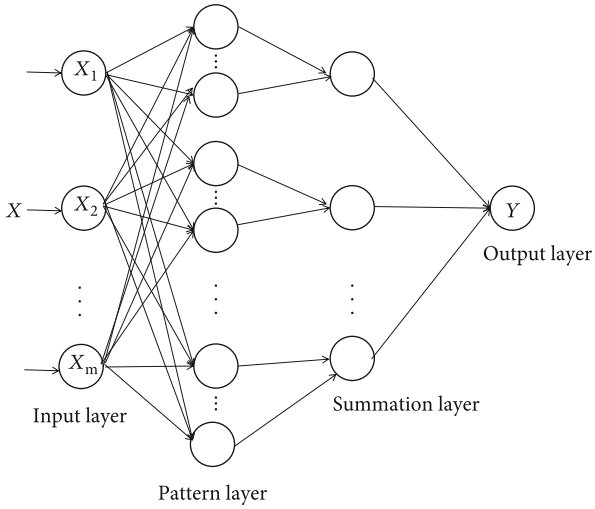

Figure 1: Structure of PNN.

2.1.1. Input Layer. Before input to the input layer, the sample data need to be standardized. The activation function in the input layer is used to introduce the sample data and calculate the distance between the input and training vectors, which is calculated by

$$d_{ij} = \left|X_k - x_{ij}\right|,$$
$$X = \begin{bmatrix} X_{11} & X_{12} & \cdots & X_{1n} \\ X_{21} & X_{22} & \cdots & X_{2n} \\ \cdots & \cdots & \cdots & \cdots \\ X_{m1} & X_{m2} & \cdots & X_{mn} \end{bmatrix} = \begin{bmatrix} X_1 \\ X_2 \\ \cdots \\ X_m \end{bmatrix}, \quad (1)$$

where X represents the standardized sample data, X_k represents the group k in sample data X, x_{ij} represents the training sample data of class i and group j, X_{ij} represents the class i and group j data in the sample data to be identified, m represents the number of groups of sample data X, and n represents the number of features in each group.

2.1.2. Pattern Layer. The number of cells in this layer is the same as that of training samples. The Gaussian function was introduced into this layer as the activation function. The distance from the input layer was used as the input in the pattern layer. The output of the pattern layer is

$$G_{ij}(X_k) = \frac{1}{(2\pi)^{1/2}\sigma^l} \exp\left(-\frac{\left(X_k - x_{ij}\right)\left(X_k - x_{ij}\right)^T}{\sigma^2}\right), \quad (2)$$

where $G_{ij}(X_k)$ represents the output value of class i and group j in the pattern layer; σ represents the smoothing factor, a key parameter for PNN training; and l represents the dimension of the sample vector.

2.1.3. Summation Layer. The number of cells in this layer is the same as the number of the PNN target classes. In this layer, the output of pattern layer was added separately based on different classes, and the output of the summation layer is as follows [36, 37]:

$$F_i(X_k) = \frac{\sum_{j=1}^{N_i} G_{ij}(X_k)}{N_i}, \quad (3)$$

where N_i is the group number of class i in the training sample and $F_i(X)$ reflects the probability that the input vector X_k is judged as class i.

2.1.4. Output Layer. The number of cells in the layer is 1. The class corresponding to the largest one in $F_i(X_k)$ was output as 1, and the rest was output as 0.

2.2. SSA. Sparrow search algorithm (SSA) is an intelligent optimization algorithm to simulate the foraging and antipredation behavior of sparrow population, which was proposed in 2020 [38]. This algorithm has the characteristics of strong optimization ability and fast convergence speed. Sparrow populations were divided into finders and followers, and the finders provided foraging directions for the followers. The sparrow population was set up with a certain percentage of sparrows aware of danger to avoid attacks, usually 10 to 20 percent. SSA is shown in Figure 2 and could be divided into seven steps as follows.

2.2.1. Set the SSA Initial Parameters. The number of sparrows, the maximum number of iterations, the ratio of discoverers to followers, the proportion of sparrows aware of danger of sparrows, and warning value are set.

2.2.2. Calculate the Fitness Function Value. The fitness function value was calculated by using the initial parameters of SSA. The fitness function is usually the error function between the estimated value and the actual one.

2.2.3. Update the Finder's Location Information Based on the Calculated Alarm Value. The position information of finders in the population was updated by using [39–41]

$$X_{ij}^{k+1} = \begin{cases} X_{ij}^k \exp\left(-\dfrac{i}{a^* \mathrm{iter}_{\max}}\right), & R_2 < \mathrm{ST}, \\ X_{ij}^k + \mathrm{QL}, & R_2 \geq \mathrm{ST}, \end{cases} \quad (4)$$

where k represents the current number of iterations; $\mathrm{iter}_{\max}$ represents the maximum number of iterations; X_{ij}^k represents the position information of the ith sparrow in the jth dimension of the sparrow population; R_2 represents a random number ranging from 0 to 1; ST represents the early-warning value initially set, generally 0.5 to 1; Q represents a random number subject to normal distribution; and L represents a matrix of $1 \times D$, where D represents the dimension of the sparrow population. When $R_2 < \mathrm{ST}$, that is, there are no predators around the foraging environment, the finder could perform extensive search operations; when $R_2 \geq \mathrm{ST}$, that is, some sparrows have already found predators, all sparrows need to quickly move to somewhere safe to feed.

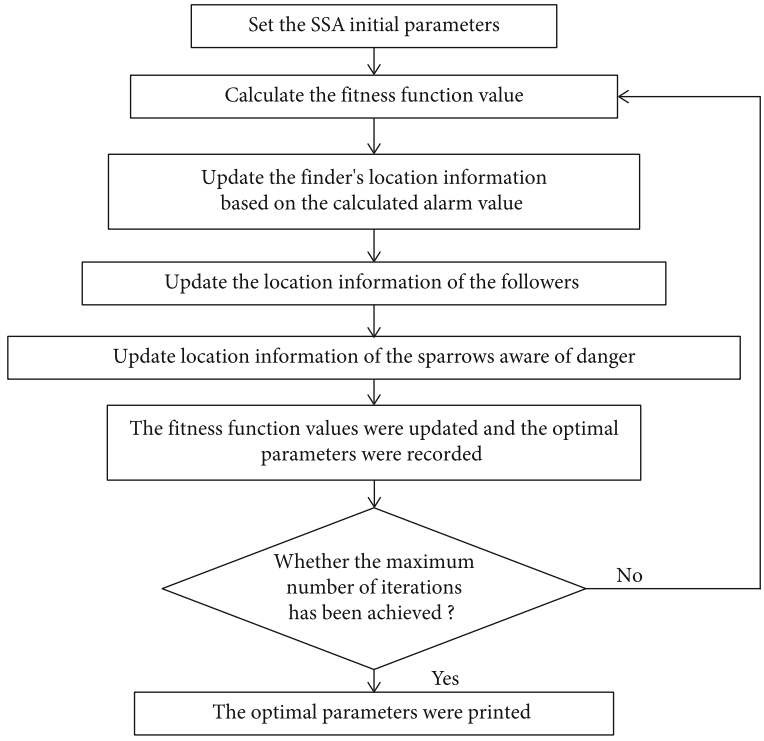

Figure 2: SSA flow chart.

2.2.4. Update the Location Information of the Followers. The position information of followers in the population was updated by using

$$X_{ij}^{k+1} = \begin{cases} Q \exp\left(\dfrac{X_{\text{worst}}^{k} - X_{ij}^{k}}{i^2}\right), & i > \dfrac{M}{2}, \\ X_F^{k+1} + \left|X_{ij}^{k} - X_F^{k+1}\right| A^{+}, & \text{else}, \end{cases} \tag{5}$$

where M represents the number of population, X_{worst}^{k} represents the worst position information in the sparrow population at the k iteration, X_F^k represents the best position information of the finders in the sparrow population at the k iteration, and A is a matrix of $1 \times d$, where each element in A is randomly assigned as 1 or -1 and $A^{+} = A^{T}(A\,A^{T})^{-1}$. When $i > M/2$, that is, the ith follower with a lower fitness value has not received food and needs to fly somewhere else to forage for food.

2.2.5. Update the Location Information of the Sparrows Aware of Danger. Update the position information of the sparrows aware of danger in the population by using

$$X_{ij}^{k+1} = \begin{cases} X_{\text{best}}^{k} + \beta\left|X_{ij}^{k} - X_{\text{best}}^{k}\right|, & F_i > F_g, \\ X_{ij}^{k} + K\left[\dfrac{\left|X_{ij}^{k} - X_{\text{worst}}^{k}\right|}{F_i - F_w + \varepsilon}\right], & F_i = F_g, \end{cases} \tag{6}$$

where X_{best}^{k} represents the optimal position information in the sparrow population at the k iteration, β represents a random number following a normal distribution, K represents a random number from -1 to 1, F_i represents the fitness value of the ith sparrow, F_g represents the current optimal fitness value, F_w represents the current value of the worst fitness, and ε represents a very small constant in preventing the denominator from returning to zero. When $F_i < F_g$, the sparrow is at the edge of the population and is extremely vulnerable to predators; when $F_i = F_g$, that is, sparrows are aware of danger and need to be close to other sparrows to minimize their risk of predation.

2.2.6. Update the Fitness Values and Record the Optimal Parameters. Using the position information of sparrow population in Equations (4), (5), and (6), the fitness values were recalculated and reordered. The fitness values and the best and worst position information of the sparrow were also recorded.

2.2.7. Whether the Maximum Number of Iterations Is Achieved. If the number of iterations does not reach the maximum number of iterations at this time, the iterative calculation will continue until the number reaches the maximum of iterations, and then, the optimal fitness value and corresponding optimal position information of the sparrow will be output.

2.3. Development of PCA-SSA-PNN Model. Based on the field data of a tunnel in western China and the data of rock burst in the diversion tunnel project of Pakistan and the

Table 1: The classification of rock burst grade [42].

Features of rock burst	Rock burst grades			
	I	II	III	IV
Sound features	None	Cracking sounds and tearing sounds	The crisp crackling sound	Very loud popping sounds
Movement features	None	Loosen or peel off	Burst, peeled off, and little ejection	Lots of bursts and ejections
Aging features	None	Occurs sporadically and intermittently	Long duration	Occurs in succession and rapidly extends deep
Influence depth	None	<0.5 m	0.5 to 1 m	1 to 3 m
Hazardous degree	None	Little	Relatively large	Serious

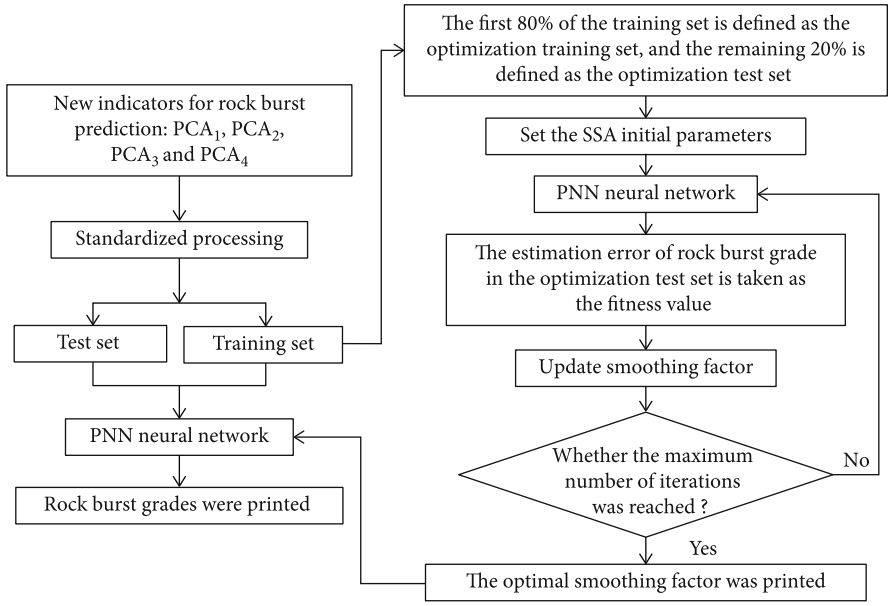

Figure 3: Structure of PCA-SSA-PNN.

Erlang Mountain tunnel of China, 43 groups of data [7, 14, 25, 26, 33] were selected. Each group of the data contains seven rock burst influencing factors, including maximum in situ stress σ_{max}, maximum tangential stress σ_θ, rock strength σ_{ci}, rock mass strength σ_{cm}, the ratio of σ_θ to σ_{ci}, the ratio of σ_{ci} to σ_{max}, and the ratio of σ_{cm} to σ_{max}. Among them, σ_{max}, σ_θ, and σ_{ci} were obtained by indoor and outdoor tests, while σ_{cm} was estimated by the Hoek-Brown strength criterion. These seven factors constitute a prediction index system of rock burst grade. Using the method of Table 1 (proposed by *National Standards Compilation Group of People's Republic of China* [42]), the classification of rock burst grade was divided into four classes: no rock burst, slight rock burst, medium rock burst, and strong rock burst, corresponding to the numbers I, II, III, and IV, respectively.

Considering that the Gaussian function in the PNN needs to be independent of each index of the rock burst prediction, the principal component analysis (PCA) method was used to reduce the dimension of the seven indexes of rock burst grade prediction, and four new independent indexes of rock burst grade prediction were obtained: PCA_1, PCA_2, PCA_3, and PCA_4. Figure 3 shows the structure of the new multi-index rock burst grade prediction method PCA-SSA-PNN. The original and new predicted indexes are shown in Table 2.

As shown in Figure 3, the 43 groups of new index data of rock burst in Table 2 were standardized by

$$x_s = \frac{x_p - \bar{x}_p}{x_{ps}}, \tag{7}$$

where x_s represents the standardized data, x_p represents new index data of rock burst, and $\bar{x}_p$ and $x_{p\sigma}$ represents the mean value and variance of the new index data of rock burst, respectively.

The 29 of the 43 groups of new index data were randomly selected as the training set, and the remaining 14 groups were selected as the test set. The smoothing factor σ is a key parameter in determining the performance of PNN. The network is easy to be overfitted if the smoothing factor is too small, while the details may be impossible to be distinguished if the smoothing factor is too great [43]. In the current study, the SSA was used to optimize the smooth factor in the PNN, the training set was again divided

Table 2: Rock burst data.

No. of samples	Original index of rock burst prediction							New index of rock burst prediction				Rock burst grade
	σ_{ci}	σ_{max}	σ_{cm}	σ_{θ}	σ_{cm}/σ_{max}	σ_{ci}/σ_{max}	$\sigma_{\theta}/\sigma_{ci}$	PCA_1	PCA_2	PCA_3	PCA_4	
1	40.62	49.7	2.42	97.63	0.05	0.82	2.40	-9.82	12.67	-4.26	-5.51	IV
2	35.63	23.5	2.12	63.5	0.09	1.52	1.78	-89.75	-11.16	-2.43	0.14	III
3	84.54	22.2	4.1	77.74	0.18	3.81	0.92	0.62	48.54	-5.87	5.06	II
4	30.43	34.8	1.47	69.3	0.04	0.87	2.28	-76.55	9.80	-5.14	-2.80	IV
5	22.15	19.9	1.51	53.3	0.08	1.11	2.41	152.31	21.20	7.08	3.40	III
6	21.08	43.3	1.02	100.84	0.02	0.49	4.78	-96.69	-24.31	-1.32	-0.86	IV
7	26.51	31.8	1.2	91.49	0.04	0.83	3.45	-49.84	27.83	-7.36	-4.06	IV
8	43.49	28.6	2.11	55.92	0.07	1.52	1.29	-4.07	34.42	-3.91	-1.71	III
9	101.27	31	3.72	87.78	0.12	3.27	0.87	126.53	-46.30	9.27	5.08	III
10	62.88	33.3	2.66	96.78	0.08	1.89	1.54	123.80	-53.88	5.52	5.43	III
11	100.97	45.4	5.25	128.19	0.12	2.22	1.27	112.39	-1.58	-3.57	-6.35	III
12	43.15	36.6	2.09	102.18	0.06	1.18	2.37	-67.53	16.71	-5.44	-8.31	IV
13	123.03	48.6	8.42	124.53	0.17	2.53	1.01	-56.15	-33.90	0.44	10.88	III
14	78.87	28.8	3.57	80.44	0.12	2.74	1.02	1.37	51.01	-8.43	5.21	III
15	88.76	29.6	4.31	78.42	0.15	3.00	0.88	112.51	0.23	-4.60	-6.13	III
16	41.1	28.7	2.13	74.24	0.07	1.43	1.81	1.05	52.59	-4.10	5.27	III
17	74.83	24.9	3.16	70.21	0.13	3.01	0.94	112.59	-2.02	-2.44	-6.54	III
18	48.4	35.8	2.69	101.45	0.08	1.35	2.10	153.85	28.37	9.71	3.51	III
19	63.97	78.7	3.32	206.68	0.04	0.81	3.23	-64.88	9.74	-4.86	-3.00	IV
20	50.37	25.4	2.8	64.74	0.11	1.98	1.29	-36.29	-39.64	0.26	-0.89	III
21	55.39	36.9	3.08	98.63	0.08	1.50	1.78	111.20	-3.45	-2.19	-6.20	III
22	42.54	46.3	2.21	121.1	0.05	0.92	2.85	115.40	5.76	-2.58	-6.68	IV
23	132.64	88.9	4.45	238.75	0.05	1.49	1.8	132.22	-31.42	7.20	4.79	IV
24	136.26	88.9	5.95	239.82	0.07	1.53	1.76	114.73	3.43	-3.58	-6.64	IV
25	138.53	88.9	7.27	239.66	0.08	1.56	1.73	1.15	52.67	-3.98	5.23	IV
26	130.79	88.9	5.24	239.35	0.06	1.47	1.83	-62.49	-52.63	1.31	4.22	IV
27	128.45	88.9	6.34	238.92	0.07	1.44	1.86	-0.52	46.59	-6.98	5.32	IV
28	130.31	88.9	6.32	239.77	0.07	1.47	1.84	-98.72	-15.03	-2.23	6.51	IV
29	136.46	54.9	7.67	121.45	0.14	2.49	0.89	-55.89	-31.71	-0.85	-2.98	III
30	141.58	54.9	10.43	120.34	0.19	2.58	0.85	-123.82	22.46	24.15	-2.50	III
31	141.67	54.9	10.56	120.42	0.19	2.58	0.85	-3.66	37.64	-5.36	5.37	III
32	137.91	54.9	8.13	121.36	0.15	2.51	0.88	136.03	-22.35	2.09	4.70	III
33	140.79	54.9	5.92	121.08	0.11	2.56	0.86	-54.77	-11.16	-3.13	-4.46	III
34	135.84	54.9	6.74	120.90	0.12	2.47	0.89	56.89	-51.74	2.07	-2.60	III
35	126.23	54.9	7.10	121.18	0.13	2.30	0.96	-83.62	-23.39	-1.53	-0.06	III
36	118.95	110	7.74	262.88	0.07	1.08	2.21	-62.86	19.60	-5.41	-1.73	III
37	108.54	110	11.54	262.67	0.10	0.99	2.42	-54.94	-26.42	-1.00	-3.58	III
38	171.24	110	22.45	262.00	0.20	1.56	1.53	-89.54	-32.39	-0.57	7.65	II
39	84.98	110	6.70	262.59	0.06	0.77	3.09	0.18	47.11	-6.13	5.07	III
40	92.48	110	11.51	262.64	0.10	0.84	2.84	-83.61	61.48	42.32	-4.27	III
41	164.4	110	18.85	263.04	0.17	1.49	1.6	-72.71	-43.18	-0.04	-3.16	II
42	66	9.1	33.00	25.40	3.63	7.25	0.38	-54.54	-19.06	-1.52	-1.67	I
43	114	18.1	57.00	48.32	3.15	6.30	0.42	-111.56	-33.10	-0.58	-0.18	I

into optimization training set and optimization test set, and the estimated loss value of rock burst grade in optimization test set was calculated. The estimated loss value was minimized by constantly updating the smooth factor, and the optimal smooth factor value was then recorded and output, and the optimum smooth factor was finally input into the PNN to obtain the rock burst grade by using the prediction network PCA-SSA-PNN.

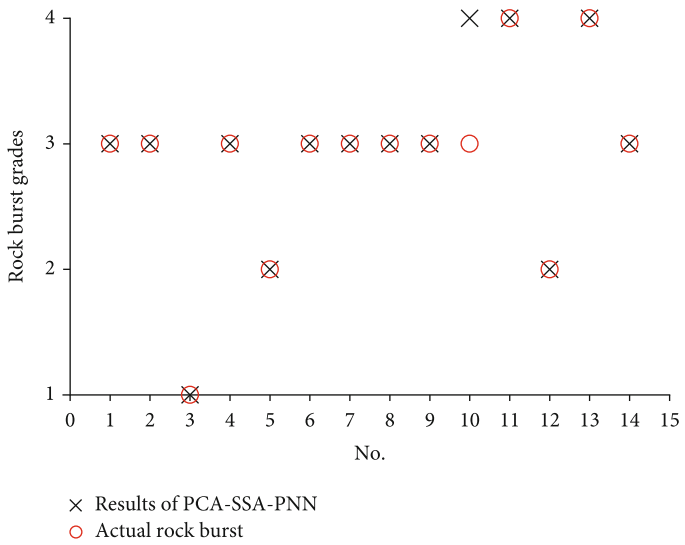

Figure 4: Prediction results of PCA-SSA-PNN.

3. Evaluation of PCA-SSA-PNN-Based Architecture

3.1. Prediction Results of PCA-SSA-PNN-Based Architecture. The new rock burst index data in Table 2 were utilized as the original data set of rock burst grade prediction network, and the total errors of training set and test set were considered as the fitness function value of rock burst grade prediction network. The SSA was used to optimize the PNN, and the optimal smoothing factor (1.0217) was obtained. Therefore, a multi-index rock burst grade prediction network based on PCA-SSA-PNN was constructed. The PCA-SSA-PNN-based architecture was adopted to predict the rock burst grades of the test set. Figure 4 shows the prediction results.

It can be seen from Figure 4 that there is a misjudgment in group 10 of the test data set, and the prediction was one grade higher than the actual rock burst, with an error ratio of less than 8%; the prediction results of PCA-SSA-PNN-based architecture are generally consistent with the actual rock burst grades. In order to further analyze the performance of PCA-SSA-PNN, the statistical results in Figure 4 are shown in Table 3.

Table 3 shows the comparison between the prediction results of PCA-SSA-PNN and actual grades in detail. It can be seen from Table 4 that the PCA-SSA-PNN has a higher prediction accuracy of no rock burst, slight rock burst, and strong rock burst with the accuracy ratios of 100%; the prediction accuracy of PCA-SSA-PNN for medium rock burst is close to 90%, which could meet the needs of engineering; the PCA-SSA-PNN may overestimate the medium rock burst by 11.11%; the average overprediction ratio of rock burst prediction by PCA-SSA-PNN is less than 8%; the PCA-SSA-PNN does not underestimate the rock burst grades; the average accuracy of rock burst prediction by PCA-SSA-PNN reaches 90% (here 92.86%), indicating that the established PCA-SSA-PNN has strong ability in estimating rock burst grades.

Table 3: Prediction results of various rock burst grades.

Evaluation of prediction results	Rock burst grades			
	I	II	III	IV
Accuracy ratio	100%	100%	88.89%	100%
Overprediction ratio	0%	0%	11.11%	0%
Underprediction ratio	0%	0%	0%	0%
Error ratio	0%	0%	11.11%	0%
Average accuracy ratio	92.86%			
Average overprediction ratio	7.14%			
Average underprediction ratio	0%			
Average error ratio	7.14%			

3.2. Comparison between PCA-SSA-PNN and Other Prediction Methods. In exploring the feasibility of the above-established PCA-SSA-PNN for estimating rock burst grades, three single-index methods, or Russenes' [6], Barton's [8], and Xu et al.'s [25, 26] methods, were conducted to estimate the rock burst grade for the test set data. The single-index prediction methods are shown in Table 4. Furthermore, four multi-indexes, or back propagation (BP) neural network, support vector machine (SVM), random forest (RF), and standard PNN (smoothing factor is set to 0.5), were also conducted to estimate the rock burst grades.

It can be seen from Table 4 that in predicting the rock burst grades, Barton's and Russenes' methods are based on the rock strength, while Xu et al.'s method is based on the rock mass strength. Considering the consistency in comparison, the cases of σ_{cm}/σ_{max} greater than 0.15 were considered as minor rock burst.

Using these above single- and multi-index prediction methods, the rock burst grade predictions were obtained (see Table 5).

The statistics of prediction results of rock burst grades by using the single- and multi-index prediction methods are conducted and shown in Table 6.

As shown in Table 6,

(a) for the comparison of PCA-SSA-PNN and single-index prediction methods, Barton's method and

Table 4: Single-index prediction methods of rock burst grade.

Single-index prediction methods	Indicators	Rock burst grade			
		I	II	III	IV
Barton's method	σ_{ci}/σ_{max}	>10	5 to 10	2.5 to 5	<2.5
Russenes' method	$\sigma_{\theta}/\sigma_{ci}$	<0.2	0.2 to 0.3	0.3 to 0.55	<0.55
Xu et al.'s method	σ_{cm}/σ_{max}	>0.15		0.07 to 0.15	<0.02

Table 5: Results by various rock burst prediction methods.

No.	Single-index methods						Multi-index methods									Actual rock burst
	σ_{ci}/σ_{max}	$\sigma_{\theta}/\sigma_{ci}$	σ_{cm}/σ_{max}	Barton	Russenes	Xu et al.	PAC1	PAC1	PAC1	PAC1	BP	SVM	RF	Standard PNN	PCA-SSA-PNN	
1	2.22	1.27	0.12	IV	IV	III	112.39	-1.58	-3.57	-6.35	III	III	IV	I	III	III
2	1.98	1.29	0.11	IV	IV	III	-36.29	39.64	0.26	-0.89	III	III	III	III	III	III
3	6.3	0.42	3.15	II	III	II	111.56	33.10	-0.58	-0.18	I	I	I	I	I	I
4	3.01	0.94	0.13	III	IV	III	112.59	-2.02	-2.44	-6.54	III	III	III	III	III	III
5	1.49	1.6	0.17	IV	IV	II	132.22	31.42	7.20	4.79	III	III	II	II	II	II
6	1.52	1.78	0.09	IV	IV	III	-4.07	34.42	-3.91	-1.71	III	III	III	III	III	III
7	3.27	0.87	0.12	III	IV	III	126.53	46.30	9.27	5.08	III	III	III	III	III	III
8	2.53	1.01	0.17	III	IV	II	-56.15	33.90	0.44	10.88	III	III	III	III	III	III
9	0.84	2.84	0.10	IV	IV	III	-83.61	61.48	42.32	-4.27	IV	III	IV	III	III	III
10	0.77	3.09	0.06	IV	IV	IV	0.18	47.11	-6.13	5.07	II	III	IV	I	IV	III
11	1.47	1.83	0.06	IV	IV	IV	-62.49	52.63	1.31	4.22	IV	IV	IV	IV	IV	IV
12	3.81	0.92	0.18	III	IV	III	0.62	48.54	-5.87	5.06	III	III	III	III	II	II
13	0.82	2.4	0.05	IV	IV	IV	-9.82	12.67	-4.26	-5.51	IV	IV	IV	IV	IV	IV
14	2.56	0.86	0.11	III	IV	III	-54.77	11.16	-3.13	-4.46	III	III	III	III	III	III

Table 6: The statistical results of Table 5.

Prediction methods		Performances			
		Overprediction ratio (%)	Underprediction ratio (%)	Accuracy ratio (%)	Error ratio (%)
Single-index	Barton's method	57.1	0	42.9	57.1
	Russenes' method	85.7	0	14.3	85.7
	Xu et al.'s method	21.4	7.1	71.5	28.5
Multi-index	BP	21.5	7.1	71.5	28.5
	SVM	14.2	0	85.8	14.2
	RF	28.5	0	71.5	28.5
	Standard PNN	7.1	14.3	78.6	21.4
	PCA-SSA-PNN	7.1	0	92.9	7.1

Table 7: Rock burst grade prediction of Mufeiling tunnel.

No.	Mileage	σ_{ci} (MPa)	σ_{cm} (MPa)	σ_{max} (MPa)	σ_{θ} (MPa)	σ_{ci}/σ_{max}	$\sigma_{\theta}/\sigma_{ci}$	σ_{cm}/σ_{max}	Rock burst grade	
									Prediction	Actual
1	DK77+500	68.93	2.69	28.6	68.59	2.41	0..99	0.094	III	III
2	DK79+050	68.93	2.69	36.5	91.85	1.89	1.33	0.074	III	III

Russenes' method are based on the rock strength and have the poorer performances with the prediction accuracy less than 50%, and Xu et al.'s method is based on the rock mass strength and has a better performance with the prediction accuracy of greater than 70%, while the established PCA-SSA-PNN in this study has the best performance; Russenes' method may overestimate the rock bursts grade in

most cases, followed by Barton's, Xu et al.'s, and PCA-SAA-PNN methods

(b) for the comparison of single- and multi-index prediction methods, the underprediction ratio of the rock burst is very low and much lower than the overprediction ratio both by the single- and multi-index methods; compared with the single-index prediction methods, the multi-index prediction methods have higher accuracy ratio and lower overprediction ratio; among the single-index methods, Xu et al.'s method has the highest accuracy, reaching 71.5%, while among the multi-index methods, BP method has the lowest accuracy, also reaching 71.5; the average accuracy of multi-index methods is higher than that of single-index methods, so the predictions by the multi-index methods are closer to the actual rock burst grades

(c) for the comparison of PCA-SSA-PNN and other multi-index prediction methods, PCA-SSA-PNN has the highest prediction accuracy, followed by SVM, standard PNN, BP, and RF; the predictions by established PCA-SSA-PNN are much closer to the actual rock burst grade than those by other four multi-index methods; all of the five multi-index methods overestimate the rock burst grade with the great-small overestimating ratio of RF, BP, SVM, standard PNN, and PCA-SSA-PNN; PCA-SSA-PNN, SVM, and RF do not underestimate the rock burst grade, while BP and standard PNN may underestimate the grades; the standard PNN-based architecture underestimates the rock burst grades, while that of PCA-SSA-PNN-based architecture is greatly improved both with the accuracy ratio increasing by 14.3% and with the underprediction ratio reducing to zero

In conclusion, the multi-index methods is more suitable for the prediction of rock burst grade than the single-index prediction methods; compared with the other four multi-index rock burst prediction methods, the established PCA-SSA-PNN is more reasonable to predict the grade classification of rock burst.

4. Discussions

In order to analyze the performance when the proposed model face with the new conditions, a new rock burst case was introduced. Mufeiling tunnel of Hangzhou-Wenzhou railway is located in Tonglu County, Hangzhou City, Zhejiang Province, China. The starting mileage is DK74 +702.93, the ending mileage is DK84+943.27, and the central mileage is DK79+823.08, with a total length of 10240.34 m. The tunnel site is located in the middle and low mountainous area, with large relief and natural slope of 25~35°. The highest elevation of the tunnel site is about 889 m, and the maximum depth is 619 m. According to statistics, rock bursts have occurred 421 times on six working faces during the construction of the Mufeiling tunnel.

Rock burst has caused serious damage to Mufeiling tunnel, increased the difficulty of the initial support and the amount of engineering, and seriously hindered the construction progress. Therefore, it is necessary to determine the rock burst grade of Mufeiling tunnel in order to take appropriate preventive measures. PCA-SSA-PNN was used to predict rock burst at DK77+500 and DK79+050 locations of Mufeiling tunnel, respectively, and the results are shown in Table 7.

It can be seen from Table 7 that the predicted results are basically consistent with the actual rock burst grades. The rock burst grade prediction method based on PCA-SSA-PNN has been well applied in Mufeiling tunnel.

5. Conclusions

In this work, the field data of a tunnel in western China and the rock burst data of the Pakistan diversion tunnel project and the Erlang Mountain tunnel project in China were used as the original input data in the rock burst prediction network. Different influencing factors of rock burst were considered to establish the index system for the rock burst grade prediction. The principal component analysis (PCA) was used to reduce the dimension of the rock burst data set and eliminate the linear correlation among different influencing factors. The sparrow search algorithm (SSA) was used to optimize the smoothing factor in the probabilistic neural network (PNN), and a multi-index rock burst prediction network PCA-SSA-PNN was thereafter obtained. The comparison of the prediction results by PCA-SSA-PNN with those by the single- and other multi-index rock burst prediction methods was furthermore conducted, respectively. It shows the following:

(1) Among the single-index rock burst prediction methods, the method considering the strength of rock mass has higher prediction accuracy

(2) The accuracy of multi-index methods is often higher than that of single-index methods in predicting the grade classification of rock burst

(3) Among the multi-index rock burst prediction methods, in the order from large to small, the overprediction rates are random forest, back propagation, support vector machine, standard PNN, and PCA-SSA-PNN, while the underprediction rates are RF, BP, standard PNN, SVM, and PCA-SSA-PNN

(4) The established rock burst prediction method based on the PCA-SSA-PNN architecture considers the influence of rock mass strength, and the rock burst grade estimated by the method is in good agreement with the actual rock burst grade, which could be used for the rapid prediction of rock burst in practice

The multi-index rock burst grade prediction method established in this study takes into account the influence of rock mass strength on rock burst. However, the rock mass strength cannot be directly obtained by testing methods at

present, so it is often estimated by empirical formula, and there may be errors between estimated results and actual values. Moreover, the number of different rock burst grades in PCA-SSA-PNN training is small, which will have some influence on the generalization ability of the network. Therefore, the category and quantity of rock burst grade data need to be increased in the subsequent research, and the selection method of rock mechanical characteristic parameters and the application range of the new multi-index prediction method also need to be further studied.

Data Availability

Some or all data, models, or code that support the findings of this study are available from the corresponding author upon reasonable request.

Conflicts of Interest

The authors declare that there is no conflict of interest.

Acknowledgments

Financial support for the study was provided by the Science and Technology Project of Henan Province under Grant No. 222102320204.

References

[1] A. Y. Cao, Y. Q. Liu, S. Q. Jiang et al., "Numerical investigation on influence of two combined faults and its structure features on rock burst mechanism," *Minerals*, vol. 11, no. 12, p. 1438, 2021.

[2] G. Q. Chen, M. C. He, and F. S. Fan, "Rock burst analysis using DDA numerical simulation," *International Journal of Geomechanics*, vol. 18, no. 3, article 04018001, 2018.

[3] Z. L. Li, L. M. Dou, G. F. Wang, W. Cai, J. He, and Y. L. Ding, "Risk evaluation of rock burst through theory of static and dynamic stresses superposition," *Journal of Central South University*, vol. 22, no. 2, pp. 676–683, 2015.

[4] H. Y. Yi, Z. H. Ouyang, X. X. Zhou et al., "Study on the modification of confining rock for protecting coal roadways against impact loads from a roof stratum," *Minerals*, vol. 11, no. 12, p. 1331, 2021.

[5] M. Zhang, "Classification prediction of rockburst in railway tunnel based on hybrid PSO- BP neural network," *Geofluids*, vol. 2022, Article ID 4673073, 8 pages, 2022.

[6] B. F. Russenes, *Analyses of Rock Burst in Tunnels in Valley Sides (in Norwegian)*, Norwegian Institute of Technology, Trondheim, Norway, 1974.

[7] L. S. Xu and L. S. Wang, "Research on the rock mechanics of rock burst disasters in Erlangshan tunnel," *Highway*, vol. 12, no. 12, pp. 6–8, 2000.

[8] N. Barton, R. Lien, and J. Lunde, "Engineering classification of rock masses for the design of tunnel support," *International Journal of Rock Mechanics and Mining Sciences*, vol. 6, no. 4, pp. 189–236, 1974.

[9] S. Afraei, K. Shahriar, and S. H. Madani, "Statistical assessment of rock burst potential and contributions of considered predictor variables in the task," *Tunnelling and Underground Space Technology*, vol. 72, pp. 250–271, 2018.

[10] J. Q. He, M. Q. Lin, X. Q. Liu et al., "New method for introducing gradient stress into rock-burst prediction," *Chinese Journal of Geotechnical Engineering*, vol. 356, no. 11, pp. 136–143, 2020.

[11] F. Y. Wu, C. He, B. Wang, J. B. Zhang, W. Meng, and J. S. Liu, "Study on the classification of rockburst intensity of Lasa-Linzhi railway based on stress criterion," *Journal of Southwest Jiaotong University*, vol. 56, no. 4, pp. 792–803, 2021.

[12] S. M. Wang, J. Zhou, C. Q. Li, D. J. Armaghani, X. B. Li, and H. S. Mitri, "Rockburst prediction in hard rock mines developing bagging and boosting tree-based ensemble techniques," *Journal of Central South University*, vol. 28, no. 2, pp. 527–542, 2021.

[13] S. L. Qiu, X. T. Feng, C. Q. Zhang, and T. B. Xiang, "Estimation of rockburst wall-rock velocity invoked by slab flexure sources in deep tunnels," *Canadian Geotechnical Journal*, vol. 51, no. 5, pp. 520–539, 2014.

[14] W. Z. Chen, C. S. Ma, H. M. Tian, and J. P. Yang, "Discussion on rockburst predictive method applying to TBM tunnel construction," *Rock and Soil Mechanics*, vol. 38, Supplement 2, pp. 241–249, 2017.

[15] C. S. Ma, W. Z. Chen, X. J. Tan, H. M. Tian, J. P. Yang, and J. X. Yu, "Novel rockburst criterion based on the TBM tunnel construction of the Neelum- Jhelum (NJ) hydroelectric project in Pakistan," *Tunnelling and Underground Space Technology*, vol. 81, pp. 391–402, 2018.

[16] Y. Du, X. T. Zheng, M. W. Xie, Y. J. Jiang, and Q. Q. Liu, "Strength weakening characteristic of rock burst structural planes," *Chinese Journal of Engineering*, vol. 40, no. 3, pp. 269–275, 2018.

[17] E. T. Mohamad, C. S. Yi, B. R. Murlidhar, and R. Saad, "Effect of geological structure on flyrock prediction in construction blasting," *Geotechnical and Geological Engineering*, vol. 36, no. 4, pp. 2217–2235, 2018.

[18] G. L. Feng, X. T. Feng, B. R. Chen, Y. X. Xiao, and Z. N. Zhao, "Effects of structural planes on the microseismicity associated with rockburst development processes in deep tunnels of the Jinping-II hydropower station, China," *Tunnelling and Underground Space Technology*, vol. 84, pp. 273–280, 2019.

[19] H. Zhou, F. Z. Meng, C. Q. Zhang, D. W. Hu, F. G. Yang, and J. J. Lu, "Analysis of rockburst mechanisms induced by structural planes in deep tunnels," *Bulletin of Engineering Geology and the Environment*, vol. 74, no. 4, pp. 1435–1451, 2015.

[20] J. Zhou, X. Li, and X. Shi, "Long-term prediction model of rockburst in underground openings using heuristic algorithms and support vector machines," *Safety Science*, vol. 50, no. 4, pp. 629–644, 2012.

[21] L. J. Dong, L. I. Xibing, and K. Peng, "Prediction of rockburst classification using random forest," *Transactions of Nonferrous Metals Society of China*, vol. 23, no. 2, pp. 472–477, 2013.

[22] C. L. Wang, A. X. Wu, H. Lu, T. C. Bao, and X. H. Liu, "Predicting rockburst tendency based on fuzzy matter-element model," *International Journal of Rock Mechanics and Mining Sciences*, vol. 75, pp. 224–232, 2015.

[23] C. Q. Zhang, J. Yu, J. Chen, J. J. Lu, and H. Zhou, "Evaluation method for potential rockburst in underground engineering," *Rock and Soil Mechanics*, vol. 37, pp. 341–349, 2016.

[24] T. Z. Li, Y. X. Li, and X. L. Yang, "Rock burst prediction based on genetic algorithms and extreme learning machine," *Journal of Central South University*, vol. 24, no. 9, pp. 2105–2113, 2017.

[25] C. Xu, X. L. Liu, E. Z. Wang, Y. L. Zheng, and S. J. Wang, "Rockburst prediction and classification based on the ideal-

point method of information theory," *Tunnelling and Underground Space Technology*, vol. 81, pp. 382–390, 2018.

[26] J. S. Xu, J. M. Xu, and Q. L. Tu, "Prediction of rock burst based on field geostress and rock mass strength," *The Chinese Journal of Geological Hazard and Control*, vol. 29, no. 5, pp. 52–58, 2018.

[27] W. Z. Liang, A. Sari, G. Y. Zhao, S. D. McKinnon, and H. Wu, "Short-term rockburst risk prediction using ensemble learning methods," *Natural Hazards*, vol. 104, no. 2, pp. 1923–1946, 2020.

[28] F. B. Meng, S. L. Jing, X. Z. Sun, C. X. Wang, Y. B. Liang, and D. Pang, "A new approach of disaster forecasting based on least square optimized neural network," *Geofluids*, vol. 2020, Article ID 8882241, 7 pages, 2020.

[29] J. Chen, J. K. Gao, Y. Y. Pu et al., "The rock burst hazard evaluation using statistical learning approaches," *Shock and Vibration*, vol. 2021, Article ID 5576480, 11 pages, 2021.

[30] L. Gao, Z. K. Liu, and H. Y. Zhang, "Prediction of rockburst classification of railway tunnel based on hybrid PSO-RBF neural network," *Journal of Railway Science and Engineering*, vol. 18, no. 2, pp. 450–458, 2021.

[31] S. Gong, Y. Tan, and W. Wang, "Prediction and evaluation of coal mine coal bump based on improved deep neural network," *Geofluids*, vol. 2021, Article ID 7794753, 11 pages, 2021.

[32] H. X. Liu, G. Y. Zhao, P. Xiao, and Y. T. Yin, "Ensemble tree model for long-term rockburst prediction in incomplete datasets," *Minerals*, vol. 13, no. 1, p. 103, 2023.

[33] A. M. Naji, M. Z. Emad, H. Rehman, and H. Yoo, "Geological and geomechanical heterogeneity in deep hydropower tunnels: a rock burst failure case study," *Tunnelling and Underground Space Technology*, vol. 84, pp. 507–521, 2019.

[34] C. H. Wang, Q. L. Guo, and L. Jia, "Depressed brainstem auditory function in children with cerebral palsy," *Rock and Soil Mechanics*, vol. 26, no. 3, pp. 272–278, 2011.

[35] D. F. Specht, "Probabilistic neural networks," *Neural Networks*, vol. 3, no. 1, pp. 109–118, 1990.

[36] P. A. Kowalski and P. Kulczycki, "Interval probabilistic neural network," *Neural Computing & Applications*, vol. 28, no. 4, pp. 817–834, 2017.

[37] Q. Li, F. L. Wang, Y. L. Wang et al., "Adsorption behavior and mechanism analysis of siloxane thickener for CO_2 fracturing fluid on shallow shale soil," *Journal of Molecular Liquids*, vol. 376, article 121394, 2023.

[38] J. K. Xue and S. Bo, "A novel swarm intelligence optimization approach: sparrow search algorithm," *Engineering*, vol. 8, no. 1, pp. 22–34, 2020.

[39] J. Dong, Z. H. Dou, S. Q. Si, Z. C. Wang, and L. X. Liu, "Optimization of capacity configuration of wind-solar-diesel-storage using improved sparrow search algorithm," *Journal of Electrical Engineering & Technology*, vol. 17, no. 1, pp. 1–14, 2022.

[40] Q. C. Li and J. J. Wu, "Factors affecting the lower limit of the safe mud weight window for drilling operation in hydrate-bearing sediments in the northern South China Sea," *Geomechanics and Geophysics for Geo-Energy and Geo-Resources*, vol. 8, no. 2, p. 82, 2022.

[41] Q. Li, F. L. Wang, Y. L. Wang et al., "Effect of reservoir characteristics and chemicals on filtration property of water-based drilling fluid in unconventional reservoir and mechanism disclosure," *Environmental Science and Pollution Research International*, vol. 30, no. 19, pp. 55034–55043, 2023.

[42] National Standards Compilation Group of People's Republic of China, *GB 50287-2016 Code for Hydropower Engineering Geological Investigation*, China Planning, Beijing, China, 2016.

[43] G. L. Zhang, C. L. Yang, and J. L. Wang, "Discrimination of exo-atmospheric targets based on optimization of probabilistic neural network and ir multispectral fusion," *Journal of Electronics & Information Technology*, vol. 36, no. 4, pp. 896–903, 2014.